ISSN 1069-3513, Izvestiya, Physics of the Solid Earth, 2018, Vol. 54, No. 1, pp. 52–65. © Pleiades Publishing, Ltd., 2018.
Original Russian Text © V.B. Belakhovsky, V.A. Pilipenko, Ya.A. Sakharov, V.N. Selivanov, 2018, published in Fizika Zemli, 2018, No. 1, pp. 56–68.

Characteristics of the Variability of a Geomagnetic Field for Studying the Impact of the Magnetic Storms and Substorms on Electrical Energy Systems

V. B. Belakhovsky[a], *, V. A. Pilipenko[b], **, Ya. A. Sakharov[a], and V. N. Selivanov[c]

[a] *Polar Geophysical Institute, Russian Academy of Sciences, Apatity, 184209 Russia*
[b] *Geophysical Center, Russian Academy of Sciences, Moscow, 119996 Russia*
[c] *Center of Physical and Technical Problems of the Northern Energetics, Kola Science Center, Russian Academy of Sciences, Apatity, 184209 Russia*
**e-mail: belakhov@mail.ru*
***e-mail: pilipenko_va@mail.ru*

Received December 5, 2016

Abstract—There are numerous models of geomagnetically induced currents in which the role of the main sources is allotted to the variations in the intensity of the auroral electrojet inducing the currents flowing along the latitude. Based on this it is believed that magnetic disturbances mainly threaten technological systems that are elongated in the longitudinal (W–E) direction. In this work, we make an attempt to employ new characteristics to describe the variability of the geomagnetic field during the geomagnetic storm of March 17, 2013. These characteristics, calculated from the data of the IMAGE magnetometer network stations, are compared to the records of the induced currents in the power lines on the Kola Peninsula and in Karelia. The vector technique revealed a considerably lower variability of the horizontal component of the geomagnetic field compared to its derivative. Quantitative estimates of the variability supported the fact that the variations of the field occur on a commensurate scale both in magnitude and direction. These results cannot be accounted for by the simple model of the extended ionospheric current and demonstrate the importance of allowing for small-scale current structures (with the spatial scales of a few hundred km) in the calculations of the geomagnetically induced currents. Our analysis shows that the geomagnetically induced currents are not only hazardous for the technological objects oriented in the longitudinal (W–E) direction but also for those elongated meridionally.

Keywords: geomagnetically induced currents, electric power systems, geomagnetic variations, ionospheric currents

DOI: 10.1134/S1069351318010032

INTRODUCTION

With the increasingly more extensive use of advanced technologies, their failures associated with the adverse effect of the space weather factors have become increasingly more tangible. The impacts of these factors are nowadays a natural norm people cannot avoid but should be aware of and should take into account. Among the important implications of the space weather effectsfor the ground technological systems, a prominent role is played by the geomagnetically induced currents (GICs) excited in the surface layers of the Earth and conductors during the sharp changes in the geomagnetic field. GICs may damage pipelines (Pulkkinen et al., 2001; Gummow and Eng, 2002), the main cable lines, high-voltage electric power transmission lines (EPTLs) (Boteler et al., 1998), submarine communications cables, and telephone and telegraph systems (Pirjola et al., 2005). Numerous examples are known of the catastrophic effects of GICs which took place in the United States, Canada, Scandinavia, and Japan during severe geomagnetic storms (Lanzerotti, 2001). The most intense currents (up to hundreds of A) and the strongest electric fields (>10 V/m) are excited at the auroral latitudes during the magnetic storms and substorms. The time variations of a magnetic field with $dB/dt \sim 1$ nT/s induce electric currents reaching a few A in the high-voltage electric lines in Finland; variations with $dB/dt > 40$ nT/s have led to outages in the operation of the Scandinavian EPTLs (Viljanen, 1997). The induced currents cause saturation, overheating, and even damage to the high-voltage transformers at te electric power substations (Erinmez et al., 2002). Constant expansion of energy networks, the growth of their interconnections, the increased load, and conversion to low-resistive transmission lines heighten the probability of emergencies during strong geomagnetic storms and substorms.

At the same time, even in the absence of catastrophic disruptions, GICs cause saturation of power transformers and interrupt the voltage control which

leads to transformer losses and transmission congestion. For instance, during the magnetic storms of July 15, 2000 and March 31, 2001, the energy transmission limit was reduced by 20% by the operators of the PJM electric transmission system in the United States (Forbes and St. Cyr., 2004). Simultaneously, the volume of energy transactions in the real-time market also dropped. The energy deficiency raised the regional real-time prices by almost a factor of four. The economic analysis allowing for the contributions of all possible factors shows that even relatively small magnetic storms affect real-time prices. Over as short a period as 1.5 years (June to December 2001), the space weather impact on the US energy market was about $500 000 000.

The most pronounced manifestations of the geomagnetic disturbances are observed in the auroral latitudes; therefore, in a number of (USA, Canada, Scandinavian countries), studies on the influence of GICs on the technological systems on the ground and the probable measures to mitigate these effects were launched in the 1970s. At the same time, even in the low-latitude countries, there is serious concern regarding the probable adverse impact of GICs on technological systems (Kelly et al., 2016). Based on the level and scale of investigations in this field, the Russian geophysical research overall, despite separate works (Efimov et al., 2013), clearly lags the studies conducted in the world's leading countries. Besides, in contrast to the Scandinavian countries and Canada, the auroral regions of the Russian Federation lack a sufficiently dense magnetometer network.

The correct calculation of the telluric electric fields and currents requires a sufficiently dense magnetometer network and information about the geoelectric section of the Earth's crust. There is no optimal global model of geoelectrical conductivity; therefore, various approximate schemes have to be used in the calculations. A comparison of different techniques shows that with a fairly high accuracy, telluric fields can be calculated from the simple impedance formula in the plane wave approximation and plane geometry (Vilijanen et al., 2004). The situation is largely simplified by the fact that the practically important GIC calculations operate with the integral estimates of the potential difference between the nodes of a fairly extended system (at least a few hundred km), and the required estimates can be sufficiently accurately obtained with a relatively sparse magnetometer network and a rather crude conductivity model.

Based on the calculated distribution of the telluric fields, it is possible to calculate the engineering evaluation of GICs in a given technological system with a known geometry and structure. Assessing the probable effects for each particular system is a separate problem. With the calculated responses of the potentials and currents along the specified branch pipeline or the electricity network to the GICs, engineers can gain comprehensive insight into the behavior of the cathodic protection during magnetic storms and reveal the weak points of the network. An operative forecast of the probable critical GIC thresholds can be used by the operator for reducing the rick of catastrophic consequences by lowering the load, turning on the capacitance protection systems, etc. Information about GICs is not only valuable from the practical standpoint but is also significant from the scientific point of view since GICs are an important factor in influencing solar activity on the magnetospheric–ionospheric system of the Earth.

The strongest magnetic disturbances on the ground are caused by the westward auroral electrojet inducing magnetic perturbations on the Earth's surface which are oriented along the meridian (N–S). Correspondingly, the concepts and analytical models are widespread in which the key role in GIC generation is allotted to the variations in the intensity of the auroral electrojet which induce the meridional currents (Boteler et al., 1997; Viljanen and Pirjola, 1994). Based on this it is believed that magnetic disturbances mainly threaten the technological systems (electricity lines, pipelines, etc.) that are elongated along the latitude (in the E–W direction). However, the rapid fluctuations of the magnetic field which are important for the excitation of GICs can be largely contributed by the small-scale ionospheric current structures (Viljanen et al., 2001). Hence, the variability of the geomagnetic field and the GICs induced by it should be described by more elaborate characteristics than the commonly used derivative of the N–S component of the field, dX/dt (Boteler et al., 1998).

In this work, we attempt to employ some new characteristics for describing the variability of the geomagnetic field during the magnetic storm of March 17, 2013. We used the data of the Polar Geophysical Institute (PGI) of the Russian Academy of Sciences and the Center of Physical and Technical Problems of the Northern Energetics (CPTPNE) of the Kola Science Center of the Russian Academy of Sciences on the GIC recording in the EPTLs on the Kola Peninsula and in Karelia.

SYSTEMS FOR RECORDING THE MANIFESTATION OF SPACE WEATHER AND GICS ON THE GROUND

The combined efforts of PGI and CPTPNE, have resulted in the creation in 2010 of a system for monitoring the impact of space weather on the energy system (Sakharov et al., 2007; 2009). This monitoring system, which has been continuously operating since then, incorporates five stations and is located on the Kola Peninsula and in Karelia (Fig. 1). The system records quasi-DC in the dead-grounded neutral of a power autotransformer which is connected to the EPTLs. In this work, we analyze the data from the Loukhi, Kondopoga, and Vykhodnoi substations on the 330 kV power main and Revda substation on a

110 kV power line. The coordinates and station codes are presented in Table 1. Under the development of magnetospheric disturbance, the selected set of the measurement points provides a GIC recording on the N–E striking power main.

Since it is not possible to take magnetic measurements in the immediate vicinity of the EPTLs, we used the data from the IMAGE network's magnetometers located in the region of the study (www.geo.fmi.fi/image) (Fig. 1, Table 1). By combining the magnetic observatories closest to the GIC stations, we obtain the following local station pairs: KND-HAN, LKH-OUJ, RVD-LOZ, and VHD-IVA.

Table 1. Magnetic stations

Station	Code	Geograph. latitude, N	Geograph. longitude, E
Nordkapp	NOR	71.09	25.79
Ivalo	IVA	68.70	27.30
Lovozero	LOZ	67.97	35.08
Pello	PEL	66.90	24.08
Oulu	OUJ	64.52	27.23
Hankasalmi	HAN	62.30	26.65

CHARACTERISTICS OF GEOMAGNETIC FIELD VARIABILITY

We used the following characteristics to describe the variations in the magnitude and direction of the horizontal component of the geomagnetic field. For visualizing a vector field, we can use a program that draws a sequence of snapshots of the vector field. Each snapshot is an image of the vector field at the observation points in the latitude–longitude coordinates for a given time instant. This technique is used, e.g., in the SuperMAG system for acquisition and analysis of 1-min global data of the geomagnetic field (supermag.jhuapl.edu). However, this approach will only be representative if there is a sufficiently dense two-dimensional array of magnetic stations and GIC recording points. In our case, both the GIC stations and the magnetic observatories form chains that are elongated in the meridional (N–S) direction. In this

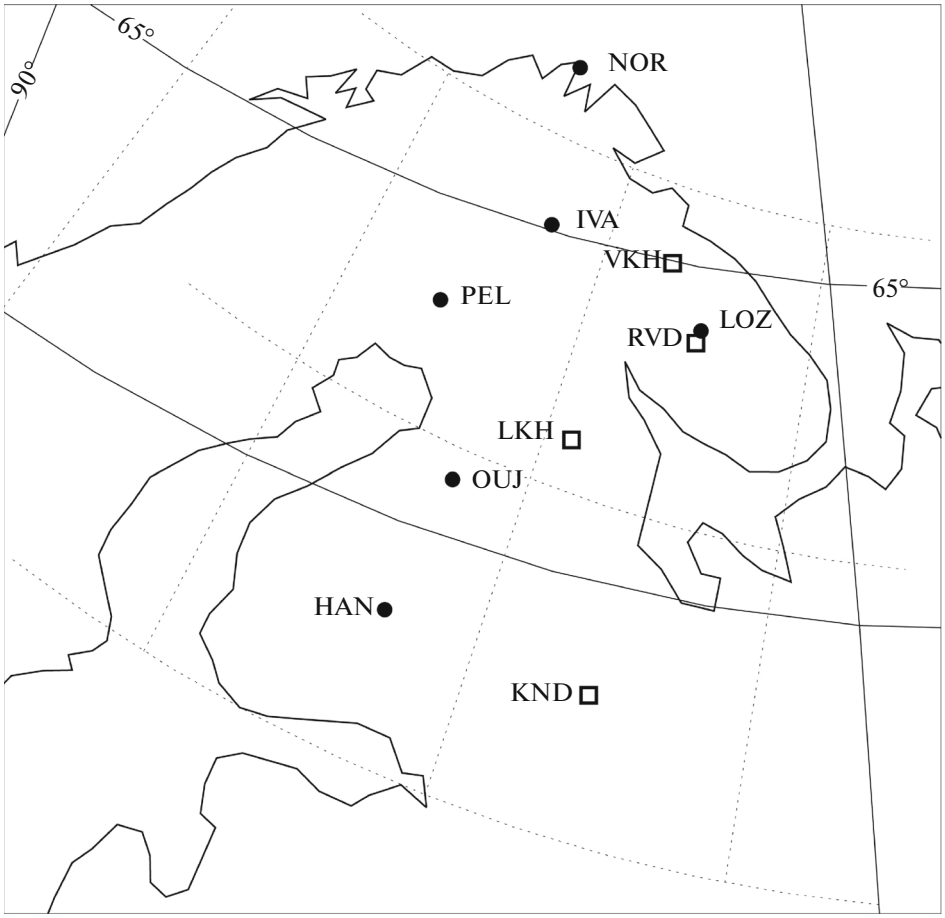

Fig. 1. Points of system of GIC measurements in EPTLs (squares) and IMAGE magnetic stations (circles). Geomagnetic coordinate grid is shown by solid line and geographic coordinate grid is shown by dashed line.

situation, it is reasonable to apply the following approaches.

Vector Diagram

The vector diagram represents, in a compact form, the time evolution of the meridional profile of the vector of magnetic disturbances. For visualizing the dynamics of the geomagnetic disturbances and ionospheric currents along the meridional profile, the geomagnetic perturbations $\Delta\mathbf{B} = \{\Delta X, \Delta Y\}$ and their vector derivatives $d\mathbf{B}/dt = \{\partial_t X, \partial_t Y\}$ for each station were plotted on a single graph in the form of disturbance vectors successively shifted in time. This technique was used, e.g., by Fries-Christensen et al. (1988) in the analysis of the ionospheric Hall vortices. The geomagnetic field disturbance was considered from the background geomagnetic field, $\Delta\mathbf{B} = \{X - X_0, Y - Y_0\}$. The derivative is calculated by the formula $\partial_t B(t) = (B(t + \Delta t) - B(t - \Delta t))/2\Delta t$.

The disturbance of the magnetic field $\Delta\mathbf{B}$ at the observation point is linked with the equivalent ionospheric current $\mathbf{J}$ above this point by the formula $\Delta\mathbf{B} = (2\pi/c)[\mathbf{J}\mathbf{x}\mathbf{n}]$ where $\mathbf{n}$ is the normal to the plane. Vector $\mathbf{J}$ is rotated by $\pi/2$ clockwise relative to $\Delta\mathbf{B}$ (however, its value will be indicated in nT).

RB Method

This method introduces the quantitative parameter *RB* which shows whether the vector field experiences variations in direction or magnitude. In the two-dimensional (2D) case, $\mathbf{B}(t) = \{X, Y\}$, parameter *RB* for the time series with length N is determined in the following way (Du et al., 2005):

$$RB = 1 - \frac{1}{N}\sqrt{\left(\sum_{i=1}^{N}\cos_x \alpha\right)^2 + \left(\sum_{i=1}^{N}\cos_y \alpha\right)^2},$$

where the magnitude of geomagnetic disturbance is $|\Delta B| = \sqrt{\Delta X^2 + \Delta Y^2}$ and the direction cosines are $\cos_x \alpha = \Delta X/|\Delta B|; \cos_y \alpha = \Delta Y/|\Delta B|$.

Parameter *RB* is independent of the intensity of the disturbance. At $RB \to 1$ the analyzed vector field experiences chaotic variations in all directions. The values of parameter $RB \to 0$ indicate that the field only varies in magnitude but not in direction.

Magnetic Storm of March 17, 2013

The magnetic storm started from the approach of the Earth's magnetosphere by the interplanetary shock wave which manifested itself on the Earth's surface by the sudden commencement (SC) pulse at ~06:00 UT (Fig. 2). At that time, the solar wind velocity sharply increased from ~400 to ~650–700 km/s. The interplanetary magnetic field became antiparallel to the geomagnetic field, thus initiating the reconnection of the fields and providing a constant energy inflow into the magnetosphere. The Dst index which characterizes the geomagnetic storm intensity dropped to –100 nT and remained at this level. At the peak of the storm (~21:00 UT), the Dst index reached –120 nT. The auroral AE index characterizing the intensity of the auroral electrojet and the substorm sharply grew to ~1000 nT and remained elevated. On March 17, 2013 overall, the AE index indicated three auroral activations: (1) immediately after the SC, the AE index started to increase and reached the maximum of ~1100 nT at ~08:00 UT; (2) the index increased after ~12:00 UT and reached the maximum of ~1000 nT at ~13:00 UT; and (3) the strongest enhancement >1800 nT occurred at ~17:00 UT.

The variations of the geomagnetic field recorded by the IMAGE magnetic stations during this storm are shown in Fig. 3. A comparison of the *X*- and *Y*-components shows that the variations in the *X*-component are stronger than in the *Y*-component, i.e., $|\Delta X| \gg |\Delta Y|$.

The system of GIC stations has recorded several noticeable bursts of GIC activity (Fig. 4). The amplitude of the first GIC peak strongly differs at the different stations (VKH ~70 A, LKH ~6 A, KND ~20 A) because these measurements are not calibrated against each other. The start of the growth in the AE index during each of the three activations corresponds to the burst in $|d\mathbf{B}/dt|$ (up to 250 nT/min) and GIC intensity (at ~06:00–08:00 UT, ~16:00 UT, and ~18:00 UT). However, the unambiguous correlation between the intensity of the substorm (characterized by the AE index) and GIC intensity is absent. For instance, despite the fact that activation (2) is commensurate in terms of the AE index with activation (1), the GICs during the second activation are far weaker. At the same time, the GIC bursts at which the AE index starts to slightly decrease are observed at ~19:00–20:00 UT and at ~21:30–23:30 UT.

A comparison of the amplitudes of magnetic disturbances ΔX and ΔY with the amplitudes of the derivatives $|dX/dt|$ and $|dY/dt|$ and the total derivative $|d\mathbf{B}/dt|$ (Fig. 5) shows that although $|\Delta X| \gg |\Delta Y|$, $|dX/dt|$ and $|dY/dt|$ are commensurate (i.e., a small ΔY does not mean that dY/dt is small) and provide a comparable contribution to the increase of $|d\mathbf{B}/dt|$. The estimates of the coefficients of correlation *R* between the GIC intensity and the amplitudes of the derivatives of the geomagnetic field for the interval 07:00–10:00 UT gives the following results: $R(|dX/dt|–|I_{GIC}|) = 0.45$, $R(|dY/dt|–|I_{GIC}|) = 0.61$, and $R(|dB/dt|–|I_{GIC}|) = 0.63$. Hence, the value of the total derivative $|dB/dt|$ is more strongly correlated to the GIC variations than the separate components, and the derivative with respect to the *Y*-component is even more closely correlated with the variations in the current than the derivative with respect to the *X*-component. On the other time intervals, the trend is similar.

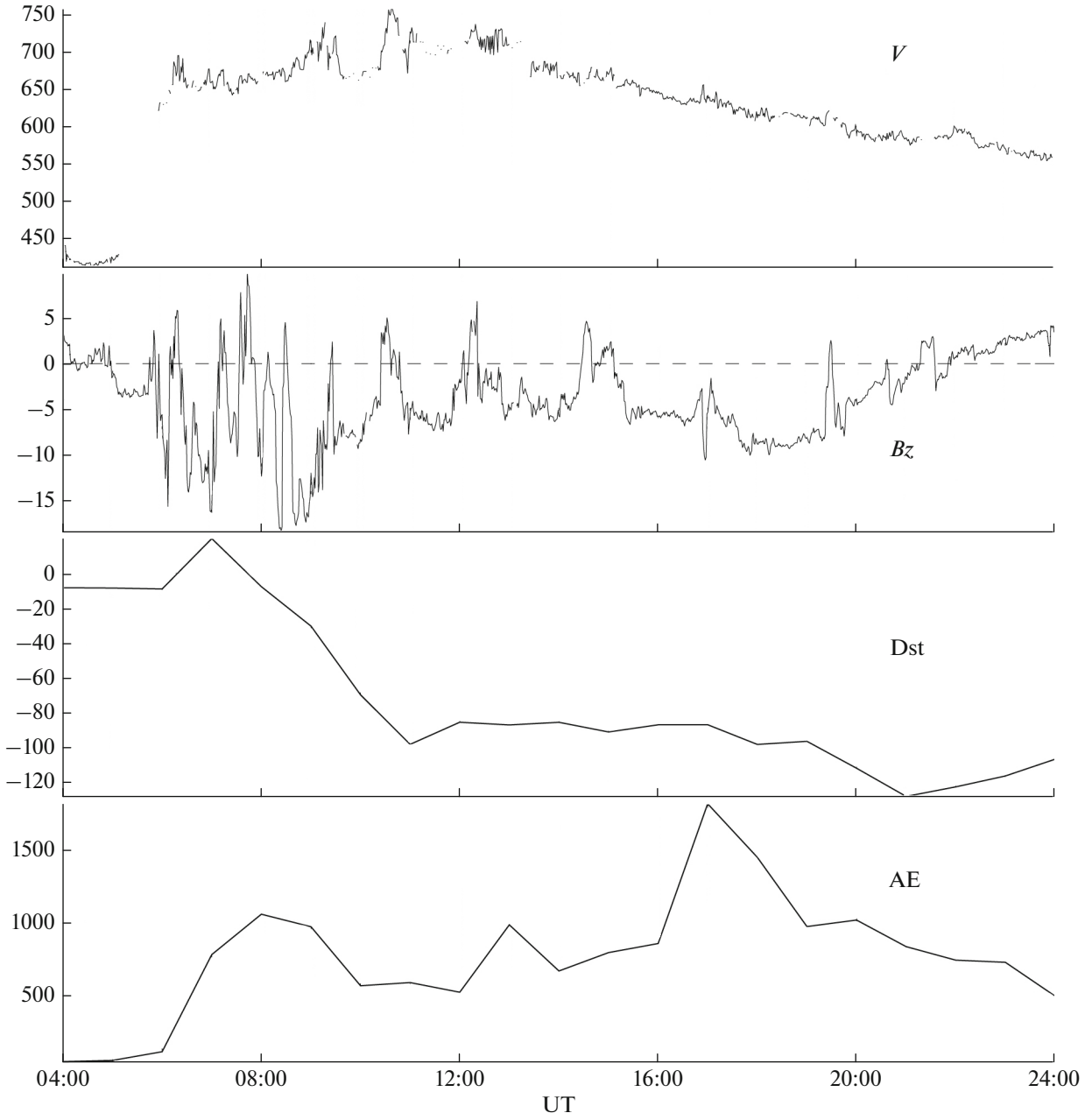

Fig. 2. Interplanetary and geomagnetic parameters during magnetic storm of March 17, 2013, 04:00–24:00 UT: solar wind (km/s), *Bz* component of interplanetary magnetic field (nT), Dst index (nT), auroral AE index (nT).

The RB parameter (Fig. 6) shows that during a magnetic storm, the geomagnetic field not only varies in magnitude but also in direction, as follows from $RB \sim 1$. Indeed, at the IVA station, this parameter varied within 0.7–0.9. The other magnetic stations give approximately the same result. Hence, the variations of the geomagnetic field cannot be fully accounted for by the variations in the intensity of the westward–eastward auroral electrojet alone.

The magnetometers used in the analysis are predominantly located longitudinally, along the geomagnetic meridian. This orientation allows us to apply the method of vector diagrams. The dynamics of the magnetic disturbances (Fig. 7) show that the variations not only occurred in the magnitude of the disturbance but also in its direction. From 06:00 to 09:00 UT, the disturbances were oriented mainly southward; subsequently, the orientation changed to the northward direction, and after 18:00 UT the vectors regained their southward orientation. These variations are caused by the strong variations in the direction of the regional ionospheric current.

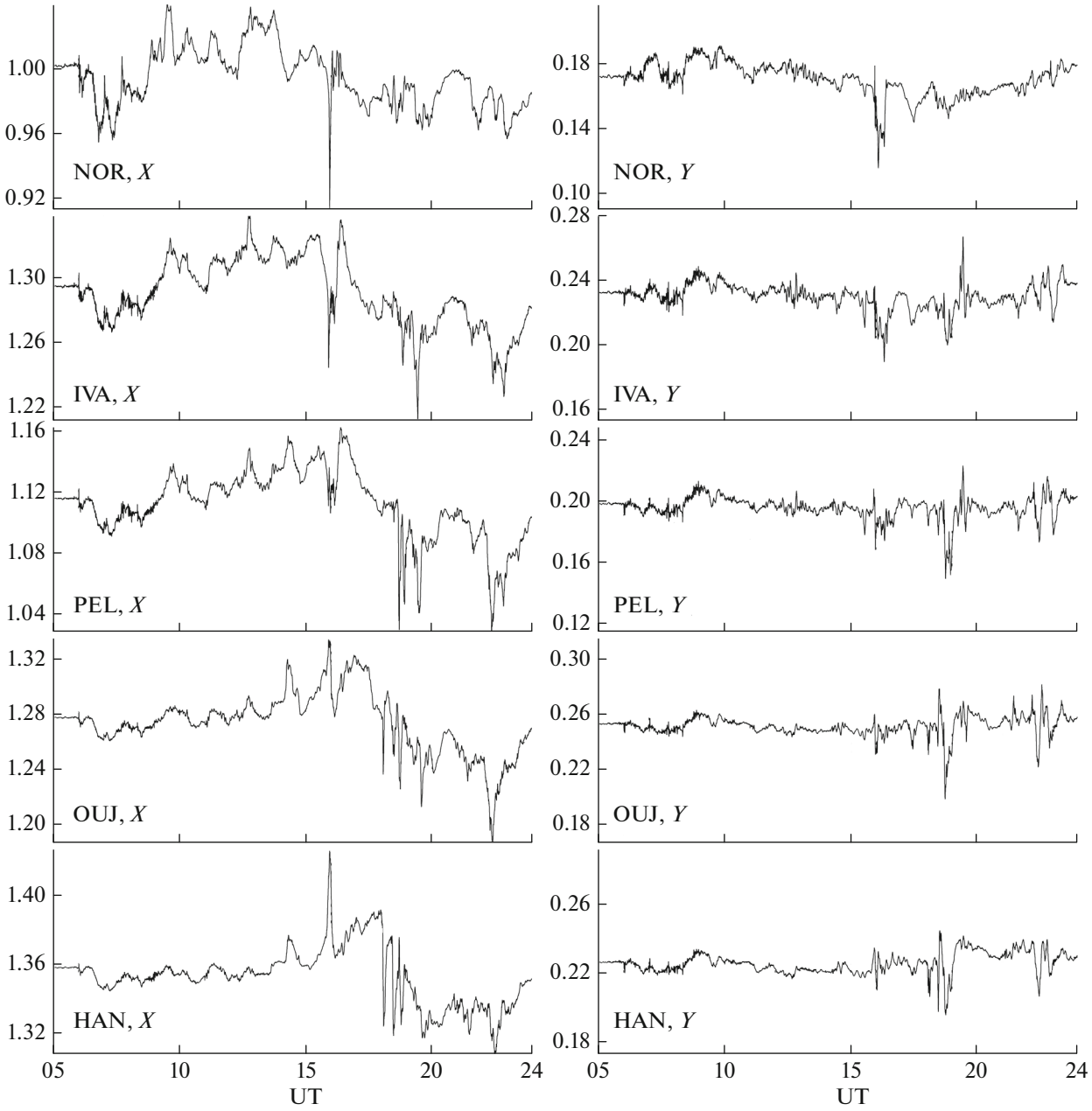

Fig. 3. Geomagnetic field ($10^4 \cdot$ nT) according to data of IMAGE magnetic stations (NOR, IVA, PEL, OUJ, HAN) during magnetic storm of March 17, 2013, 05:00–24:00 UT. Left: *X*-component; right: *Y*-component.

The distribution of the equivalent ionospheric currents (Fig. 8) shows that immediately after a SC, the currents predominantly flowed eastward and subsequently they changed to the opposite direction. In the period from 16:00 to 18:00 UT, the current flow again changed to the eastward direction. This pattern of changes appears as the transition from one vortex current system to the other. Although the large scale structure of the ionospheric currents is governed by the eastward–westward electrojet, on the smaller regional level, the currents experience strong variations in their flow direction. As a result, the GIC flow in both the N–S and W–E directions, without the predominance of any of these orientations. The data from the meridional chain of the magnetic stations allow us to estimate the longitudinal (W–E) spatial scale of the vortex current systems: it is 4.2°–4.8°, i.e., about 500 km (Fig. 9).

The orientation of GIC corresponds to the $d\mathbf{B}/dt$ rotated by 90° counterclockwise (strictly speaking, this is valid for the plane incident field and laterally homogeneous crustal conductivity). The vector diagram of the equivalent GICs constructed in the

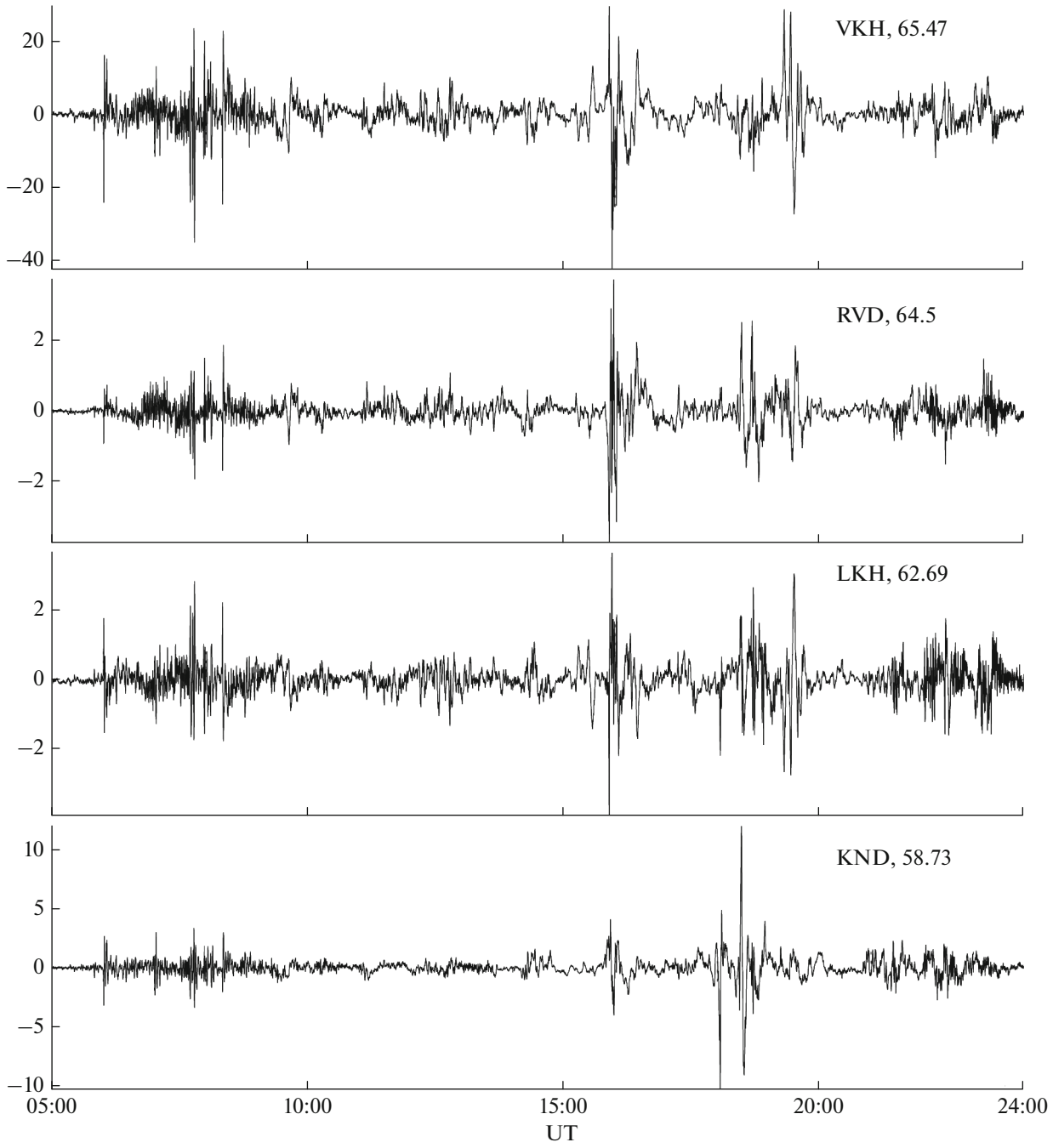

Fig. 4. Data of GIC measurement system (in A) from stations VHD, RVD, LKH, KND during magnetic storm of March 17, 2013, 05:00–24:00 UT. Geographic latitudes of recording stations are indicated after station code.

described way shows that the induced currents during bursts are oriented in all directions (Fig. 9).

DISCUSSION

Space weather manifestations such as disturbances of the geomagnetic field and ionosphere, GIC induction in the conductive constructions, outages in the radio communication and satellite navigational systems, etc., are most intense in the auroral latitudes. The total energy released during a magnetic storm of medium intensity is ~1400 GWt, which is almost double the power of all electric power stations in the United States. Serious economic consequences for the global electric power market are observed even in cases when the space weatherdoes not cause catastrophic interruptions. Forbes and St. Cyr (2004) have shown that market prices in different national electric power

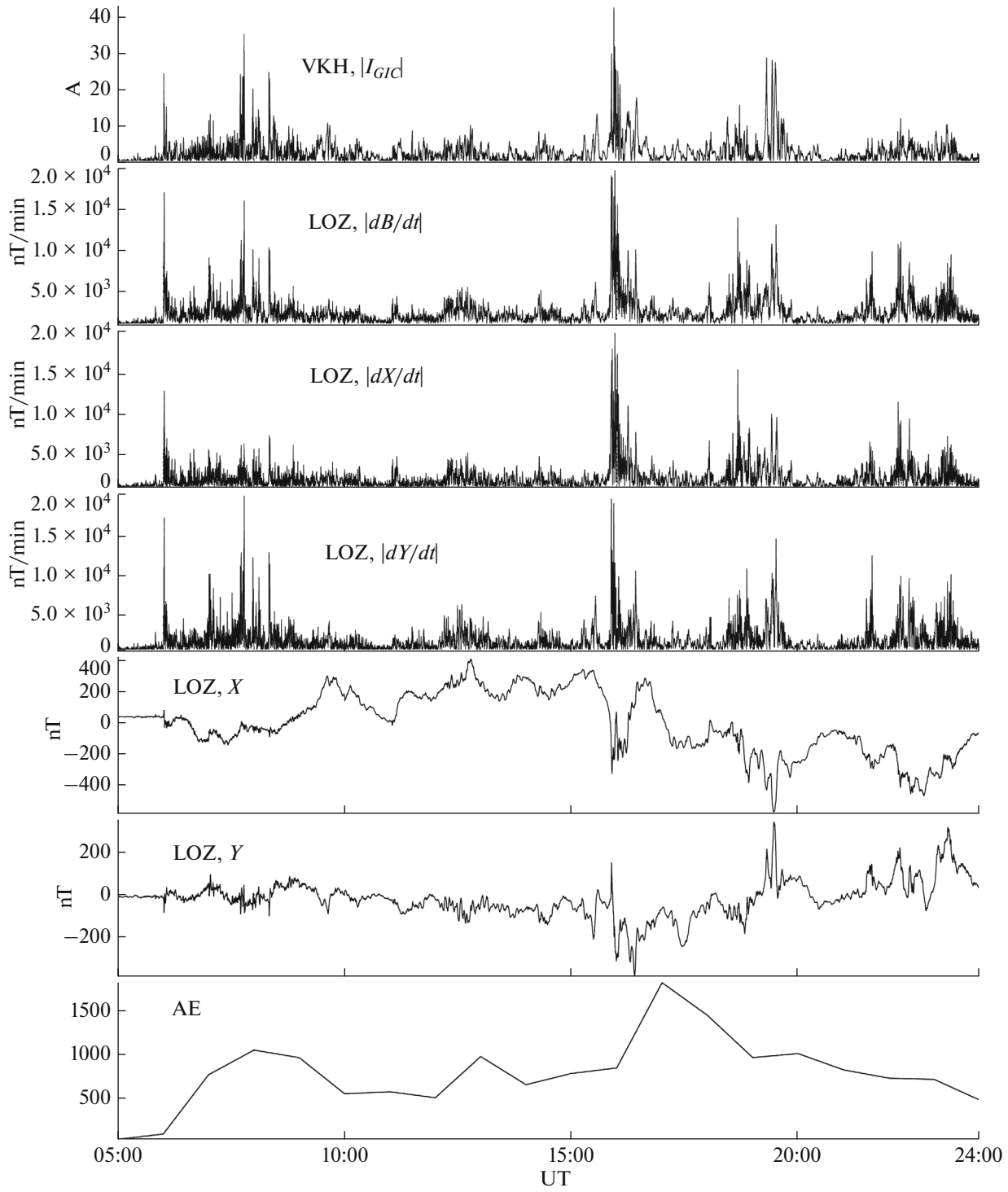

Fig. 5. Comparison of GOC amplitudes (in A), amplitudes of total derivative $|dB/dt|$ (nT/s), amplitudes of component derivatives $|dX/dt|$ and $|dY/dt|$ (nT/s), and magnetic disturbances ΔX and ΔY ($10^4 \cdot$ nT) at spatially close stations VKH and LOZ over period 05:00–10:00 UT. Variations in AE index are shown in bottom panel.

markets are statistically related to the local geomagnetic variations. Hence, even if no loss is caused to the technological equipment during a magnetic storm, the GICs induced in the regional energy systems noticeably affect the economic stability of the region. These and many other examples demonstrate the importance of a more profound study of the space weather effect on the global infrastructure.

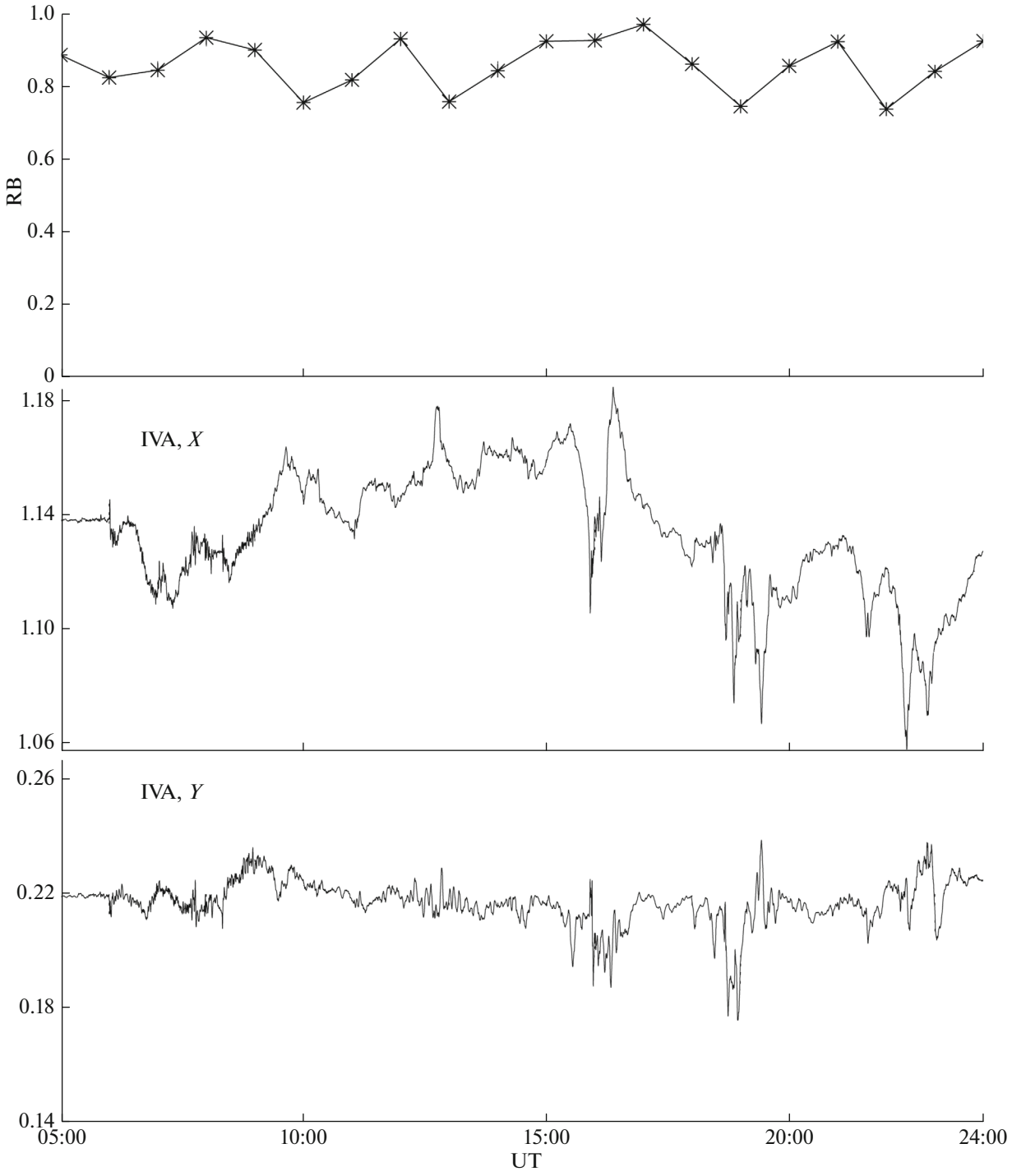

Fig. 6. Time variations of parameter RB calculated from magnetic disturbances (bottom panels) at IVA station over period from 05:00 to 24:00 UT (with step of 30 min).

These factors are critical for safe operation of the technological systems in the Arctic zone of the Russian Federation, which accommodates the most extensive oil and gas pipelines, electric power lines, and traffic arteries. Despite the utmost importance of these studies, the Russian academic community has barely touched these problems, whereas production companies in the Russian Federation are unlikely to be interested in the sustainable operation of technological systems. The calculation of the probable GIC levels at typical and extreme magnetic storms which can be used by the operators of energy networks to reduce the

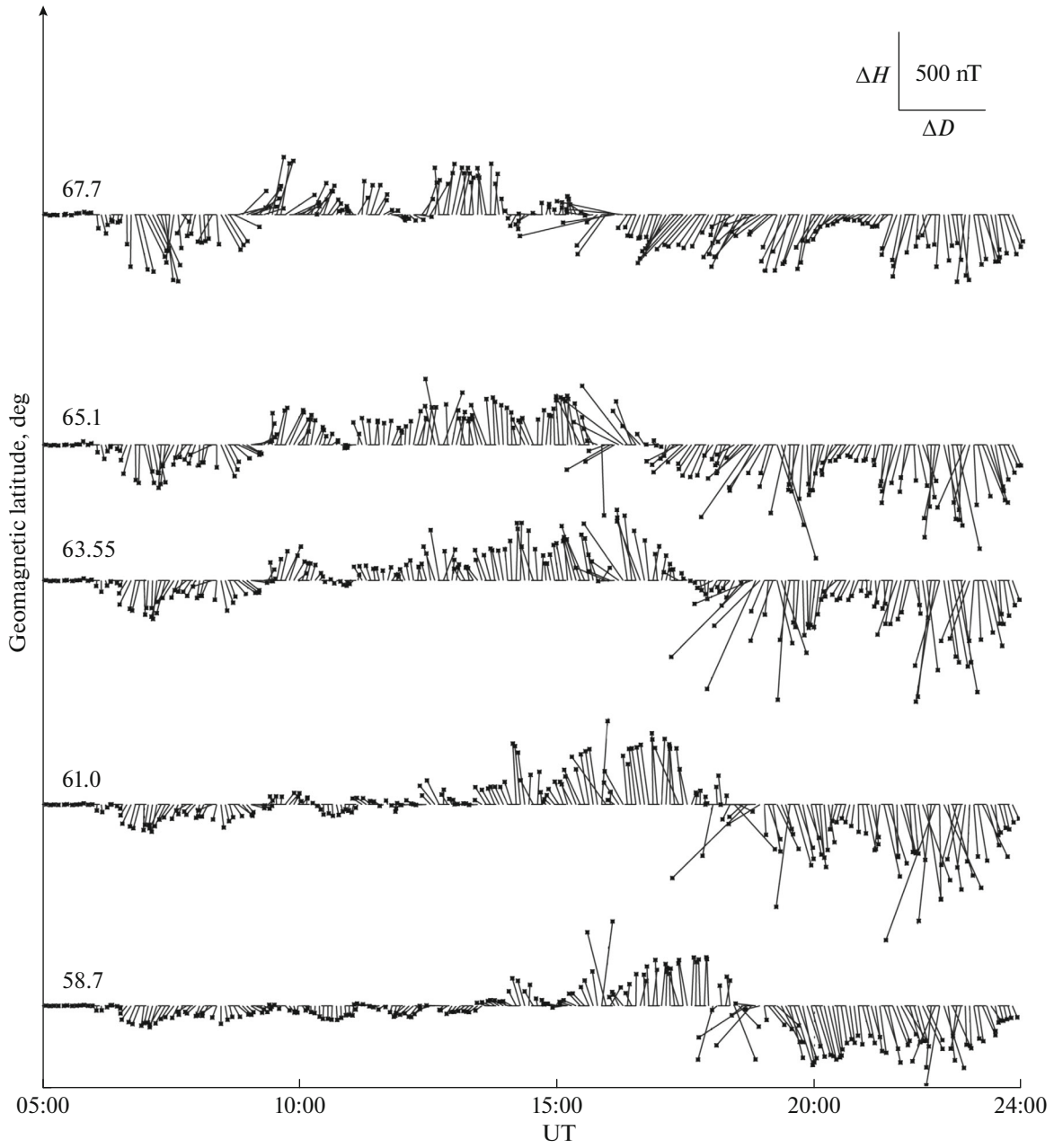

Fig. 7. Variations of magnetic disturbance vector along meridional profile (vector diagram) over period from 05:00 to 24:00 UT (with step of 5 min).

risk of catastrophic consequences is a vital and topical problem.

Meanwhile, the technologically developed countries whose territories are located in the high and low latitudes have undertaken extensive activities to create systems for monitoring and forecasting the effects of the different space weather factors on the ground-based and satellite technological systems. However, most of these initiatives are regionally specific and cannot be directly applied to the territory of the Russian Arctic. The obtained results are frequently a commercial property and inaccessible for the global scientific community. As of now, the most elaborate GIC model is the 3D model developed by Püthe and Kuvshinov (2013). This model allows calculating the GIC from large-scale sources (magnetospheric ring

Table 2. GIC recording stations

Vykhodnoi	VKH	68.83	33.08
Revda	RVD	67.77	34.99
Loukhi	LKH	65.77	31.08
Kondopoga	KND	62.21	34.28

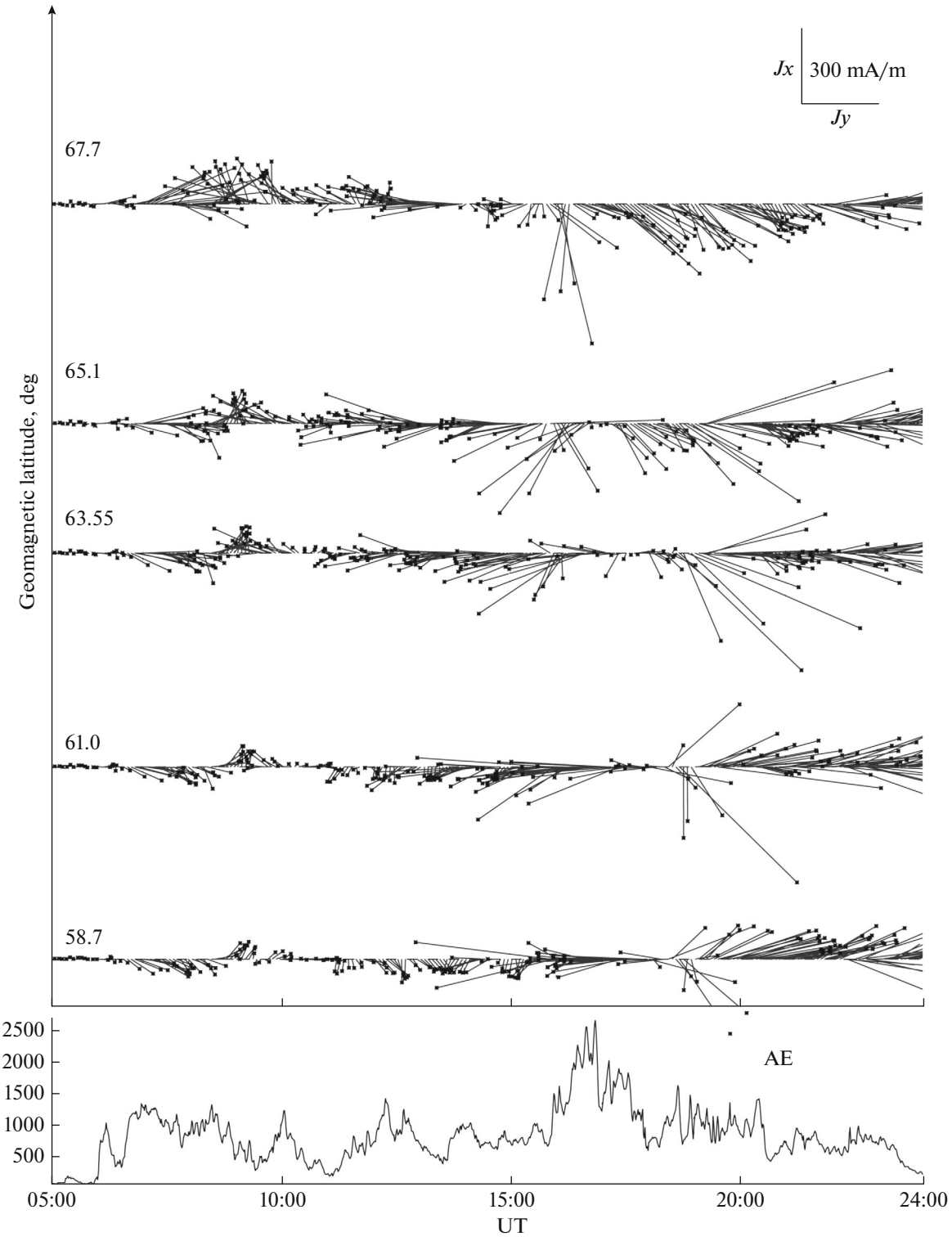

Fig. 8. Pattern of variations of equivalent ionospheric currents *J* along meridional profile over period from 05:00 to 24:00 UT (with step of 5 min). Variations of auroral AE index are shown in bottom panel.

current) in the middle latitudes (<55°) with the model conductivity of the lithosphere. The calculated peak values of the telluric electric field reach ~50 mV/km for a geomagnetic storm with a Dst of ~300 nT. However, this model cannot be used for high latitudes, where the most intense disturbances are induced by the more localized and fast substorm processes. For instance, more than 80% of the spectral power of the

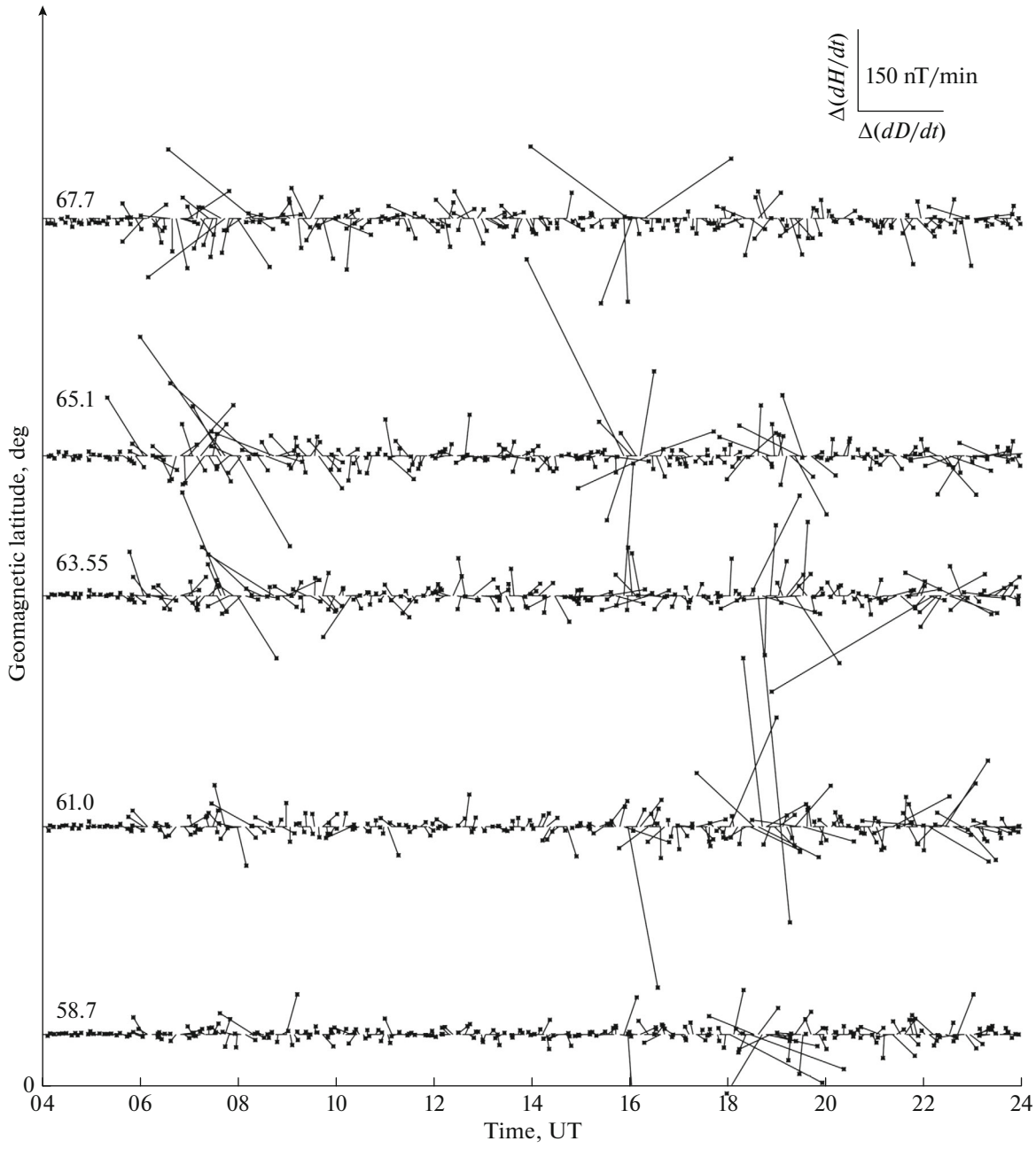

Fig. 9. $d\mathbf{B}/dt$ vector variations along meridional profile (vector diagram) over period from 05:00 to 24:00 UT (with step of 5 min).

geomagnetic field in the auroral latitudes is concentrated on time scales shorter than 8 min (Wintoff et al., 2005). The analysis of the Kola electric energy network shows that the GIC bursts predominantly occur at night during auroral substorms (Sakharov et al., 2009).

In the literature, the emergence of GICs is frequently interpreted as the result of the fluctuations in the auroral ionospheric electrojet, mainly flowing in the W–E direction. Therefore, the GIC calculations employed models in which these currents were generated by the extended eastward and westward ionospheric electrojet currents (Boteler et al., 1997; Viljanen and Pirjola, 1994). Based on these models, it was concluded that the magnetic storms and substorms predominantly affect those technological systems that are elongated in the longitudinal (W–E) direction. The vector technique for the representation of the variations of the magnetic field and its vector derivative applied by us clearly demonstrated a much higher directional variability of $d\mathbf{B}/dt$ compared to $\Delta\mathbf{B}$. The quantitative estimate of the variability, RB, supported the conclusion that the variations of the geomagnetic field occur on a commensurate scale in mag-

nitude and direction. These results show the importance of taking the small-scale current structures in the GIC calculations into account. The obtained $d\mathbf{B}/dt$ distribution cannot be interpreted by the simple model of the extended ionospheric current and requires allowance for the fields of the nonstationary vortex structures generated by the local field-aligned currents. Although the current amplitudes in these structures are relatively low and incapable of strongly affecting the $\Delta\mathbf{B}$ distribution, their time fluctuations are fairly rapid and thus they have a significant impact on the distribution of $d\mathbf{B}/dt$.

The data at our disposal were from the meridional chain of magnetic stations which only allowed us to estimate the longitudinal (W–E) dimension of the vortex current systems. Magnetic disturbances from current systems smaller than ~10^2 km will be invisible to the magnetometers on the ground. Figure 9 shows that the scale of the vortex disturbances is visually ~4.2°–4.8°, i.e., about 500 km. Stricter quantitative estimates can be derived from the numerical model. The small-scale current systems are associated with the nonstationary vortex structures created by the local field-aligned currents. In principle, the densities of the ionospheric and field-aligned currents can be estimated from the value of the magnetic disturbance. However, the GIC excitation is primarily governed by the time variation of the ionospheric current rather than by the value of the ionospheric current itself. Let us assume that the small-scale vortex current systems develop and fully disappear against the background of the auroral electrojet. We use the formula for the maximal magnetic perturbation on the ground from the Hall current vortex created by a flux tube of radius δ with the upward flowing field-aligned current $j_\parallel$ in the center and downward flowing field-aligned current at the edges (Pilipenko et al., 1999):

$$\frac{j_\parallel[\mathrm{A/m^2}]}{b^{(g)}[\mathrm{nT}]} \simeq \frac{0.1}{4\pi\delta}\left(\frac{\Sigma_P}{\Sigma_H}\right)\left(\frac{\delta+h}{\delta}\right)^2.$$

For the parameter values recorded in our experiment, $b^{(g)}$ ~500 nT, $\delta \sim 5 \times 10^5$ m, $h = 10^5$ m, and $\Sigma_H/\Sigma_P = 2$, this ratio only gives the estimate $j_\parallel \simeq 5\ \mu\mathrm{A/m^2}$.

The question concerning the ratio of a large-scale auroral electrojet and the superimposed localized current structures during the substorms remains unclear. The conclusion that the two-dimensional character of current systems cannot be ignored for GIC modeling during strong disturbances is supported by the results of Apatenkov et al. (2004). For the events with a high dB/dt value, these authors expanded the disturbance field into the contributions of an azimuthally elongated current system (electrojet) and a vortex system using the analytical approximation for the field of a line current and divergence-free current system controlled by the field-aligned current. The relative contribution of these components was then estimated. On average, the number of events with the predominant contribution of the electroject and those dominated by the vortex current is approximately equal; however, most of the rapid fluctuations with $dB/dt > 100$ nT/min (reaching $dB/dt > 900$ nT/min) were created by the vortex currents and took place in the morning. As the dB/dt variations increase, the role of the vortex structures becomes increasingly more important. The spatial scale of the vortex structures ranges from a few hundred to a thousand km. However, in our analysis, we used the 1-min data, due to which the rapid variations were averaged to a certain extent.

Thus, although the most intense magnetic disturbances on the ground are induced by the auroral electrojet and predominantly oriented in the N–S direction, in the rapid fluctuations of the magnetic field which are significant for the excitation of GICs, a noticeable contribution is made by the small-scale ionospheric current structures in which the contributions of both the horizontal components (N–S and W–E) are commensurate. This is clearly illustrated by the extreme vulnerability of the EPTLs on the Kola Peninsula to the emergence of GICs despite the fact that this network is elongated in the N–S direction. Here, it was noted that not every strong geomagnetic disturbance necessarily induces intense GICs (Sakharov et al., 2007). A clear correlation is also not revealed between the GIC intensity and geomagnetic Kp index. The unequivocal relationship between the substorm intensity and the variability of the geomagnetic field is also unlikely.

To date, promising results have been obtained in forecasting the substorm intensity characterized by the AE index based on the real-time data from interplanetary probes (Weigel et al., 2003; Wintoft et al., 2005). However, the problem of GIC forecasting is not reduced to the problem of forecasting substorms. The model required for estimating the influence of geomagnetic activity on the technological systems in the Arctic and subarctic regions should also describe, together with the dynamics of the large-scale magnetospheric–ionospheric current system, the sporadic rapidly varying localized field-aligned currents.

CONCLUSIONS

The large-scale structure of the ionospheric currents in the high latitudes is determined by the westward–eastward electrojet, which manifests itself by the predominance of the X-components of the magnetic disturbances. However, on a smaller scale regional level, the equivalent ionospheric currents and the geomagnetic disturbances induced by them experience strong variations in both magnitude and direction. As a result, the GICs flow in both the S–N and W–E directions. The vector technique for representing the variations in the horizontal component of the geomagnetic field and its time derivative has demon-

strated a much higher level of variability of $d\mathbf{B}/dt$ compared to $\Delta\mathbf{B}$. The quantitative estimate of the variability based on the RB parameter supported the fact that the variations of the geomagnetic field in magnitude and direction occur on commensurate scales. These results cannot be accounted for by the simple model of the extended ionospheric electrojet and demonstrate the importance of taking into account the fields of small-scale current structures in the calculations of GICs. Hence, GICs should be considered as an important threat to technological systems not only elongated in the longitudinal (W–E) direction but also for those oriented meridionally.

ACKNOWLEDGMENTS

The work was supported by the Russian Science Foundation (project no. 16-17-00121 (BVB, PVA)). The PGI–CPTPNE data are placed on the http://eurisgic.org website created for assessing the risk of the impact of geomagnetic disturbances on European energy systems.

REFERENCES

Apatenkov, S.V., Sergeev, V.A., Pirjola, R., and Viljanen, A., Evaluation of the geometry of ionospheric current systems related to rapid geomagnetic variations, *Ann. Geophys.*, 2004, vol. 22, pp. 63–72.

Boteler, D.H., Pirjola, R.J., and Nevanlinna, H., The effects of geomagnetic disturbances on electrical systems at the earth's surface, *Adv. Space Res.*, 1998, vol. 22, pp. 17–27.

Du, J., Wang, C., Zhang, X.X., Shevyrev, N.N., and Zastenker, G.N., Magnetic field fluctuations in solar wind, foreshock and magnetosheath: cluster data analysis, *Chin. J. Space Sci.*, 2005, vol. 25, no. 5, pp. 368–373.

Efimov, B., Sakharov, Ya., and Selivanov, V., Geomagnitnye shtormy: Issledovanie vozdeistvii na energosistemu Karelii i Kol'skogo poluostrova, *Nov. Elektrotekh.*, 2013, no. 2, p. 80.

Erinmez, I.A., Kappenman, J.G., and Radasky, W.A., Management of the geomagnetically induced current risks on the national grid company's electric power transmission system, *J. Atmos. Sol.-Terr. Phys.*, 2002, vol. 64, pp. 743–756.

Forbes, K.F. and St. Cyr, O.C., Space weather and the electricity market, *Space Weather*, 2004, vol. 2, p. S10003.

Friis-Christensen, E., McHenry, M.A., Clauer, C.R., and Vennerstroem, S., Ionospheric traveling convection vortices observed near the polar cleft: a triggered response to sudden changes in the solar wind, *Geophys. Rev. Lett.*, 1988, vol. 15, pp.235–256.

Gummow, R.A. and Eng, P., Gic effects on pipeline corrosion and corrosion-control systems, *J. Atmos. Sol.-Terr. Phys.*, 2002, vol. 64, p. 1755.

Kappenman, J.G., An overview of the impulsive geomagnetic field disturbances and power grid impacts associated with the violent sun-earth connection events of 29–31 October 2003 and a comparative evaluation with other contemporary storms, *Space Weather*, 2005, vol. 3, p. S08C01.

Kelly, G.S., Viljanen A., Beggan C., Thomson A.W.P., and Ruffenach A., Understanding GIC in the UK and French high voltage transmission systems during severe magnetic storms, *Space Weather*, 2017, vol. 15, no. 1, pp. 99–114.

Lanzerotti, L.J., Space weather effects on technologies, in *Space Weather, AGU Geophys. Monogr. Ser.*, vol. 125, Song, P., Singer, H.J., and Siscoe, G.L., Eds., Washington: AGU, 2001, pp. 11–22.

Pilipenko, V., Shalimov, S., Fedorov, E., Engebretson, M., and Hughes, W., Coupling between field-aligned current impulses and Pi1 noise bursts, *J. Geophys. Res.*, 1999, vol. 104, pp. 17419–17430.

Pirjola, R., Kauristie, K., Lappalainen, H., Viljanen, A., and Pulkkinen, A., Space weather risk, *Space Weather*, 2005, vol. 3, p. S02A02.

Pulkkinen, A., Pirjola, R., Boteler, D., Viljanen, A., and Yegorov, I., Modeling of space weather effects on pipelines, *J. Appl. Geophys.*, 2001, vol. 48, p. 233–256.

Pulkkinen, A.A., Bernabeu, E., Eichner, J., Beggan, C., and Thomson, A.W.P., Generation of 100-year geomagnetically induced current scenarios, *Space Weather*, 2012, vol. 10, p. S04003.

Püthe, C. and Kuvshinov, A., Towards quantitative assessment of the hazard from space weather. Global 3-D modellings of the electric field induced by a realistic geomagnetic storm, *Earth Planets Space*, 2013, vol. 65, p. 1017.

Sakharov, Ya.A., Danilin, A.N., and Ostafiychuk, R.M., Registration of GIC in power systems of the Kola Peninsula, *Proc. 7th Int. Symp. on Electromagnetic Compatibility and Electromagnetic Ecology*, St.-Petersburg, June 26–29, 2007, St. Petersburg, 2007, pp. 291–293.

Sakharov, Ya.A., Danilin, A.N., Ostafiychuk, R.M., Katkalov, Yu.V., and Kudryashova, N.V., Geomagnetically induced currents in the power systems of the kola peninsula at solar minimum, *Proc. 8th Int. Symp. on Electromagnetic Compatibility and Electromagnetic Ecology*, St. Petersburg, 2009, pp. 237–238.

Viljanen, A., The relation between geomagnetic variations and their time derivatives and implications for estimation of induction risks, *Geophys. Rev. Lett.*, 1997, vol. 24, pp. 631–634.

Viljanen, A., Nevanlinna, H., Pajunpaa, K., and Pulkkinen, A., Time derivative of the geomagnetic field as an activity indicator, *Ann. Geophys.*, 2001, vol. 19, pp. 1107–1118.

Viljanen, A., Pulkkinen, A., Amm, O., Pirjola, R., Korja, T., and BEAR Working Group, Fast computation of the geoelectric field using the method of elementary current systems and planar Earth models, *Ann. Geophys.*, 2004, vol. 22, pp. 101–113.

Viljanen, A., European project to improve models of geomagnetically induced currents, *Space Weather*, 2011, vol. 9, p. S07007.

Viljanen, A. and Tanskanen, E., Climatology of rapid geomagnetic variations at high latitudes over two solar cycles, *Ann. Geophys.*, 2011, vol. 29, pp. 1783–1792.

Weigel, R.S., Klimas, A.J., and Vassiliadis, D., Solar wind coupling to and predictability of ground magnetic fields and their time derivatives, *J. Geophys. Res.*, 2003, vol. 108, p. 1298.

Wintoft, P., Wik, M., Lundstedt, H., and Eliasson, L., Predictions of local ground geomagnetic field fluctuations during the 7–10 November 2004 events studied with solar wind driven models, *Ann. Geophys.*, 2005, vol. 23, pp. 3095–3101.

Translated by M. Nazarenko